Nd^{3+} sensitized Yb^{3+} luminescence in oleic acid functionalized LaF_3: $Nd^{3+}Yb^{3+}$ nanoparticles

Pramod K Nampoothiri[1*], Mayuri N Gandhi[1], Ajit R Kulkarni[2]

[1]*Centre for Research in Nanotechnology & Science (CRNTS), IIT-Bombay, Mumbai, 400076, India*
[2]*Department of Metallurgical Engineering and Materials Science, IIT-Bombay, Mumbai, 400076, India*

[*]Corresponding author: Tel: (+91) 9619589903; E-mail: pramod.nampoothiri@gmail.com

Received: 29 March 2016, Revised: 27 October 2016 and Accepted: 13 April 2017

DOI: 10.5185/amp.2017/502
www.vbripress.com/amp

Abstract

The luminescence at the absorption maximum of c-Si solar cells (1002 nm) of Ytterbium (3+) ions (Yb^{3+}) make them a suitable candidate for solar spectrum converting material for c-Si solar cell. In this work oleic acid functionalized lanthanum fluoride (OA-LaF_3) nanoparticles doped with Nd^{3+}, Yb^{3+} (2-5 nm) were synthesized by coprecipitation method in which Nd^{3+} (Neodymium (3+) ions) acts as the sensitizer for Yb^{3+}. The oleic acid chemisorption on LaF_3 nanoparticles was confirmed by FTIR and TGA analysis. OA-LaF_3: Nd^{3+} Yb^{3+} nanoparticles (Nd^{3+} -10 mol%, Yb^{3+}-0 to 20 mol%) luminescent at 880 nm, 1053 nm, 1325 nm (Nd^{3+} ions) and 1002 nm (Yb^{3+} ions) was observed for excitation at 575 nm. The excitation spectra for the Yb^{3+} emission from OA-LaF_3: Nd^{3+} Yb^{3+} showed all the excitation peaks of Nd^{3+} in the visible region. This confirmed the energy transfer from Nd^{3+} to Yb^{3+} ions. The increase in the Yb^{3+} emission intensity at 1002 nm was observed as Yb^{3+} dopant concentration increased from 0 to 5%. Above 5% of Yb^{3+} doping concentration, Yb^{3+} luminescence was observed to be decreasing, which was attributed to the concentration quenching.

Keywords: Lanthanide, downconversion, lanthanide sensitization, solar cell concentrator, oleic acid functionalization.

Introduction

Solar cells are typically composed of special light-absorbing semiconducting materials. When sunlight falls on a solar cell, the photons activate the electrons in the cell and promote them into a higher energy conduction band. One of the major factors affecting energy conversion efficiency of solar cell is the spectrum mismatch with solar light. For example crystalline Si solar cells (c-Si solar cells) work most efficiently in the 950–1100 nm spectral region, but show very low spectral absorbance to the short-wavelengths in sunlight [**1**]. This means below 950 nm and above 1100 nm the absorbance by c-Si solar cells are less efficient, which leads to loss of solar energy. This happens because the band gap of c-Si is 1.1 ev. Photons with the energy smaller than the bandgap will not get absorbed and if the photon energy is larger than the bandgap then the excess energy will be wasted by the process of thermalisation of electrons. A spectrum shifting coating which absorbs energy below 950 nm and above 1100 nm and converts to 950 nm-1100 nm can be used to solve this problem of solar spectrum mismatch [**2**]. In order to achieve that luminescence processes like upconversion, quantum-cutting, and down-converting are currently explored for developing efficient photovoltaic devices [**1-8**].

In down-converting and quantum cutting a higher energy is absorbed and converted to a lower energy. Down-converting is a process in which one higher energy photon is absorbed and converted to a lower energy photon and quantum cutting is a process in which two low energy photons are generated from one high energy photon excitation. This process would improve the efficiency of solar energy absorption, reduce the thermalisation losses and thereby result in more electron-hole pair generation. Hence, the potential of using quantum-cutting and down-converting lanthanide doped nanomaterials in solar cells has been explored in an effort to maximize their efficiency. Theoretical calculation done by Trupke *et al.* predicted an enhancement up to 38.6% in conversion efficiency for a solar cell modified with a down-converting layer [**2**].

Lanthanides comprise series of elements in the sixth row of the periodic table stretching from lanthanum to ytterbium. Lanthanide ions are luminescent by nature. They are either fluorescent (Pr^{3+}, Nd^{3+}, Ho^{3+}, Er^{3+}, and Yb^{3+}) or phosphorescent (orange Sm^{3+}, red Eu^{3+}, Gd^{3+}, which emits in the UV, green Tb^{3+}, yellow Dy^{3+}, and blue Tm^{3+}) [**4**]. Their emission covers the entire spectrum from UV to NIR. The near infrared quantum-cutting has been demonstrated in various lanthanide codoped (Ln = Tb, Tm, Pr, Er, Nd, Ho, and Dy with Yb) systems [**9-13**] and in phosphors with a single luminescent dopants (Ho^{3+}, Tm^{3+}, or Er^{3+}) [**14-16**].

Among different lanthanides, Yb^{3+} luminescence is well matching with the c-Si solar cell absorption maximum around 1000 nm. The problem with Yb^{3+} ions is Yb^{3+} ions are having an excitation state at 10000 cm^{-1}

and no energy levels in the visible region of electromagnetic spectrum. Hence Yb^{3+} ions cannot be excited by visible part of the electromagnetic spectrum. Therefore a sensitizer for Yb^{3+} ion, which will absorb in the visible region and pass that energy to Yb^{3+} ion, is essential for the use of Yb^{3+} ions as solar spectrum converter [**7, 17**]. Nd^{3+} to Yb^{3+} energy transfer has been considered and studied in several materials like of borate, metaphosphate, tellurite, and fluoroindogallate glasses [**18-22**]. Low phonon materials like LaF_3 are preferred as host materials because lower phonon energy minimizes multiphonon relaxation processes between the closely spaced energy levels of Nd^{3+}, which can reduce the radiative down conversion efficiency [**23**]. In this study Nd^{3+} ions are used as a sensitizing ion for Yb^{3+} and LaF_3 nanoparticles are used as host material.

Experimental

Materials and methods

All chemicals were used as received without any further purification. Ln $(NO_3)_3.6H_2O$ salts and Ammonium fluoride having purity of 99.99% were purchased from sigma-aldrich. Oleic acid was sourced from Merck.

Oleic acid functionalized LaF_3 nanoparticles doped with Nd^{3+} (10 mol%) and Yb^{3+} (0-20 mol%) ions were synthesized by co-precipitation route. In a typical synthesis 20 ml ethanol, in which total 0.02M of lanthanum salts ($La(NO_3)_3.6H_2O$ (0.016M, 0.52 g), $(Yb(NO_3)_3.6H_2O$ (0.002M, 0.898g), and $Nd(NO_3)_3.6H_2O$) (0.002M, 0.0877g) and oleic acid was dissolved (solution A). Ammonium fluoride (0.06M, 0.222 g) was dissolved in 80 ml distilled water (solution B). The pH of the solution B was adjusted to 10 by adding ammonium hydroxide and heated up to 70 ^oC. Further solution A was added to the heated solution B and kept at 70 ^oC for 10 minutes under stirring. The nanoparticles precipitated out and were washed several times with ethanol and dried under ambient conditions.

Characterization

The NIR fluorescence spectra were acquired using Jobin yvon fluorolog spectrofluorometer. Bruker 3000 Hyperion Microscope with Vertex 80 FTIR System was used for obtaining FTIR spectra. PERKIN ELMER, USA Diamond TG/DTA was used for obtaining the TGA plots of the samples.

Results and discussion

The morphological investigation of OA-LaF_3: $Nd^{3+}Yb^{3+}$ nanoparticles were carried out with HRTEM (**Fig. 1(a)**). The nanoparticles were dispersed in chloroform and drop caste on a 400 meshed carbon coated copper grid. The nanoparticles were spherical in shape with an average size of 5 nm. The XRD patterns of OA-LaF_3: $Nd^{3+}Yb^{3+}$ nanoparticles and standard data are shown in **Fig. 1 (b)**. The peak positions and intensities of the XRD patterns of nanoparticles were in good agreement with the PDF card data. Hence confirmed that the nanoparticles were well crystalline and exhibited hexagonal phase.

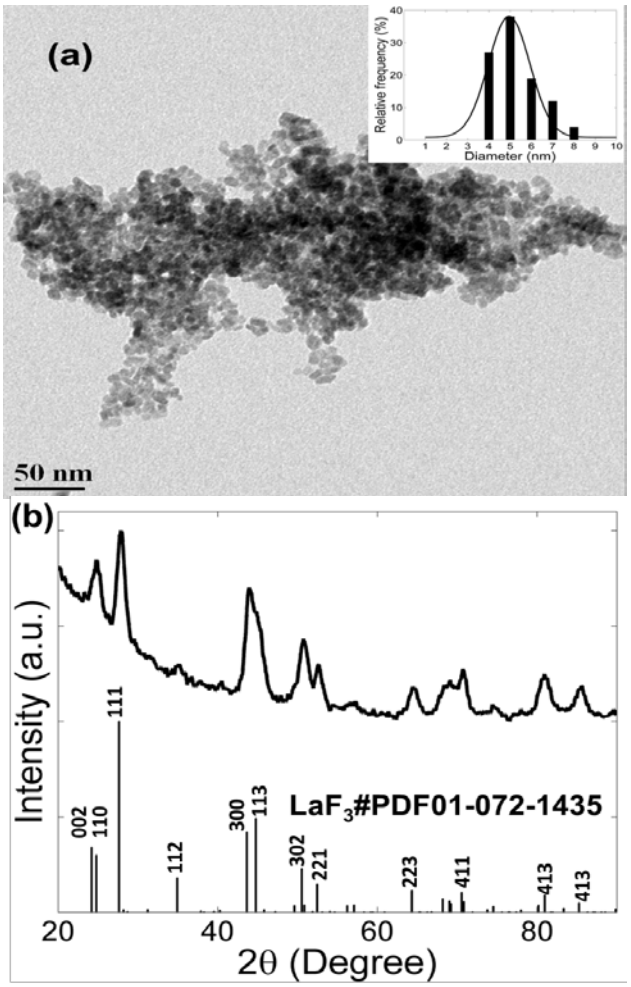

Fig. 1. HRTEM image and XRD spectra of oleic acid functionalized LaF_3 nanoparticles.

In the NIR-emitting lanthanide ions (Nd^{3+}, Er^{3+}, Yb^{3+}), the energy gap of the radiative (f–f) transition matches well with the energy of the first and second vibrational overtones of O–H and C–H groups (with vibrational quanta $\nu = 2$ and $\nu = 3$). Therefore the efficiency of the lanthanide ion luminescence would be severely quenched by the resonance energy transfer from the lanthanide ion to the molecular stretching vibrations of C–H and O–H groups present in the surrounding. Lanthanide-doped nanoparticles have a high proportion of dopant ions in the surface which would be in proximity to the quenching molecules like water. This would form of a non-radiative pathway for the excited energy and lead to the quenching of luminescence. The ions in the interior of the nanoparticles also could transfer the absorbed energy to the surface through adjacent dopant ions and result in no radiative decay. Hence, to remove OH- ions from the proximity of the lanthanide nanoparticle amphiphilic molecules like oleic acids are used [**24**]. Such amphiphilic molecules has got hydrophilic and hydrophobic ends. The hydrophilic end chemisorbs to the surface of nanoparticle and hydrophobic end at the other end replaces OH- ions from the proximity of nanoparticle surface. The adsorption of oleic acid to the nanoparticle surface was studied by FTIR and TGA analysis.

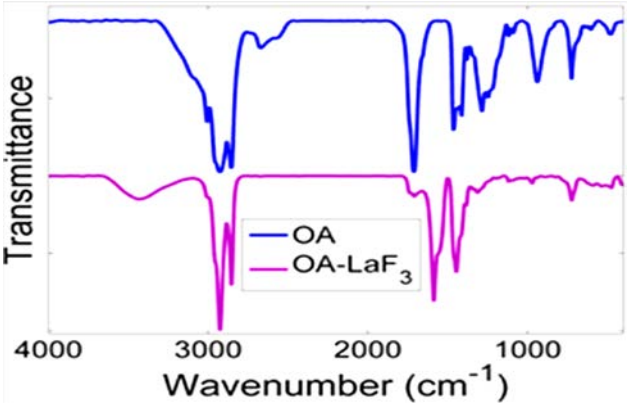

Fig. 2. FTIR spectra of oleic acid and oleic acid functionalized nanoparticles.

FTIR spectrum of oleic acid and nanoparticles functionalized with oleic acids was analyzed and confirmed the functionalization of oleic acid on nanoparticle surface (**Fig. 2**) [**25-26**]. The 1709 cm^{-1} absorption of C=O stretching was significantly reduced for all nanoparticles functionalized with fatty acids and two new bands of stretching vibrations of carboxylate anions at 1450 cm^{-1} (symmetric, ν_{sym}) and 1582 cm^{-1} (asymmetric, ν_{asym}) were observed. This confirmed the chemisorption of fatty acids on LaF_3 nanoparticle surface. The absorption observed at 2960 cm^{-1} was attributed to the asymmetric stretch vibrations of alkyl chain terminal CH_3 group and 723 cm^{-1} to the existence of $(CH_2)n$ (n <4) alkyl chains.

The type of interaction between lanthanide ion and carboxylate moiety of oleic acid could be understood by the wave number separation between symmetric and asymmetric stretching of carboxylate anions IR absorption bands. The largest Δυ (200-320 cm^{-1}) corresponds to a monodentate interaction, the medium range Δυ (140-190 cm^{-1}) indicates a symmetric coordinative bidentate interaction, and the smallest Δυ (<110 cm^{-1}) corresponds to a multidentate interaction. From FTIR spectrum of nanoparticles, the Δυ was calculated as ~132 cm^{-1} which indicated more of a symmetric coordinative bidentate interaction between carboxylate moity and nanoparticle surface [**25-28**].

The adsorption of oleic acid to the nanoparticle surface was expected to improve thermal stability of oleic acid as more energy is required for degrading these molecules. TGA measurements were carried out in nitrogen atmosphere from room temperature to 550 ^oC at 10 ^oC/min (**Fig. 3** (a)). The free oleic acid thermal degradation was observed to be starting (onset temperature) at 210 ^oC which was right shifted to 330 ^oC in the case of oleic acid functionalized nanoparticles. The peak maximum temperature in the derivative plot of TGA thermograms ((**Fig. 3** (b)) of oleic acid and nanoparticles functionalized with oleic acids also showed a right shift compared to the degradation of oleic acid. This improvement in the stability of oleic acid confirmed the efficient adsorption of oleic acid molecules on the nanoparticle surface.

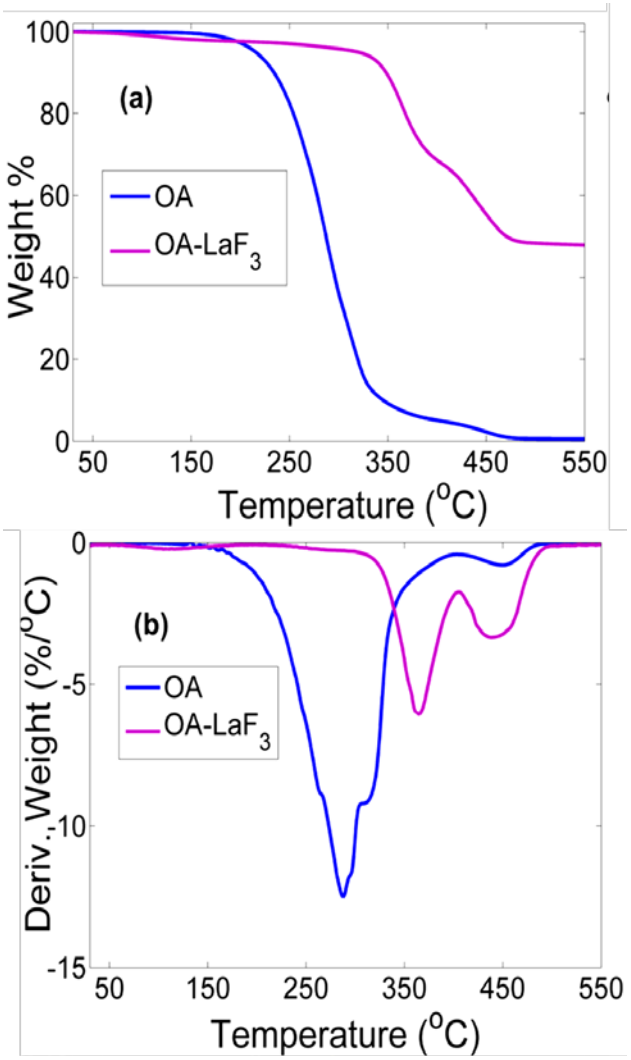

Fig. 3. The TGA thermogram (a) & DTGA (b) of OA-LaF_3: Nd^{3+} Yb^{3+} nanoparticles.

The LaF_3 nanoparticles doped with Nd^{3+} ions were excited with 575 nm and observed luminescence at 880 nm, 1053 nm and 1325 nm. These emissions were assigned to the energy transitions from $^4F_{3/2}$ to $^4F_{9/2}$, $^4F_{7/2}$ and $^4F_{13/2}$ correspondingly. Further, the luminescence from LaF_3: $Nd^{3+}Yb^{3+}$ nanoparticles were studied. Yb^{3+} ions do not have any energy states in the visible region of the electromagnetic spectrum. Hence Yb^{3+} ions cannot be excited at 575 nm at which Nd^{3+} ions could be excited. For understanding the energy transfer from Nd^{3+} to Yb^{3+}, Nd^{3+} ions were excited at 575 nm. The LaF_3: $Nd^{3+}Yb^{3+}$ nanoparticles showed Yb^{3+} emission at (1002 nm, $^2F_{5/2}$ to $^4F_{7/2}$) along with the three emissions of Nd^{3+} ion at 880 nm, 1053 nm and 1325 nm. The luminescence emission intensity from Nd^{3+} ions started to decrease as Yb^{3+} concentration increased. This was attributed to the energy transfer from Nd^{3+} to Yb^{3+} ions and concentration quenching effect. The increase in the Yb^{3+} emission intensity was observed as Yb^{3+} dopant percentage increased up to 5% (**Fig. 4** (a)).

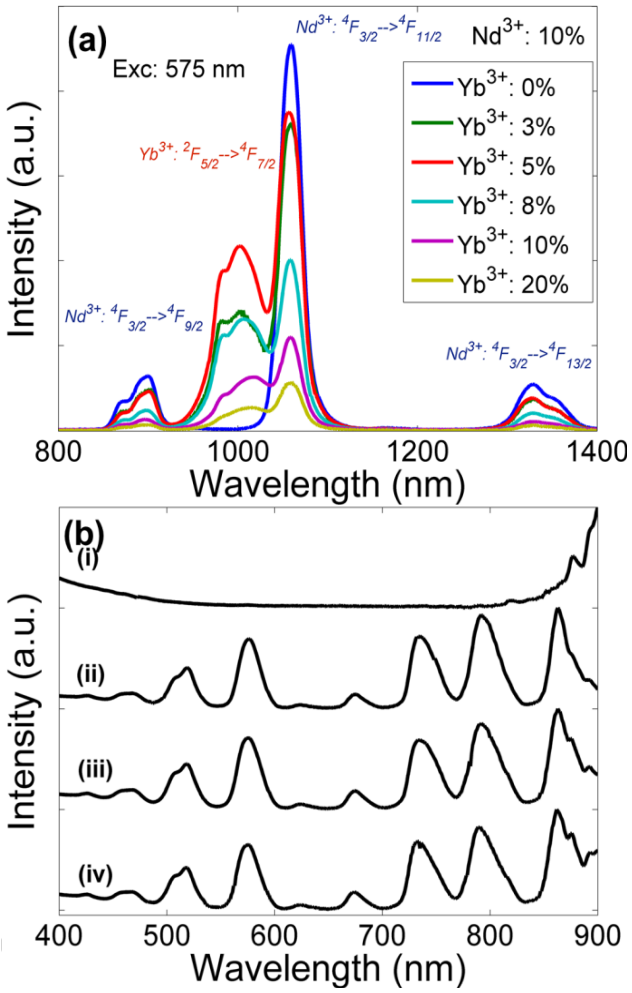

Fig. 4. (a) Fluorescence emission spectra of LaF_3: Nd^{3+} Yb^{3+} nanoparticles and (b) excitation spectra of Yb^{3+} (for emission 1002 nm) and Nd^{3+} (for emission 1053 nm) when individually doped (i & ii) and Yb^{3+} codoped with Nd^{3+} (iii & iv) in LaF_3 nanoparticles.

Above 5% of Yb^{3+} co-doped with Nd^{3+} (10 mol%), both Nd^{3+} and Yb^{3+} luminescence observed to be decreasing. This decrease of luminescence intensity could be attributed to the concentration quenching effect. As the Yb^{3+} doping percentage increased, the probability of transferring excited energy through the dopant ions to a defect or quenching ion increased. So as dopant percentage increased, the probability for the non-radiative decay of excited energy increased. It should be noted that for zero Nd^{3+} concentration both Nd^{3+} and Yb^{3+} emissions were absent in the emission spectrum when excited with 575 nm. **Fig. 4 (b)** shows excitation spectra of Yb^{3+} (for emission 1002 nm) and Nd^{3+} (for emission 1053 nm) when individually doped and Yb^{3+} codoped with Nd^{3+} in LaF_3 nanoparticles. Since Yb^{3+} ions do not have any energy states above 10000 cm^{-1}, excitation spectra of LaF_3: Yb^{3+} did not show any peaks between wavelengths 400 nm and 800 nm. In the case of Yb^{3+} codoped with Nd^{3+}, the excitation spectra for Yb^{3+} emission showed all the excitation peaks of Nd^{3+} ion in the visible region. This confirmed the energy transfer from Nd^{3+} to Yb^{3+} ions in OA-LaF_3: $Nd^{3+}Yb^{3+}$ nanoparticles.

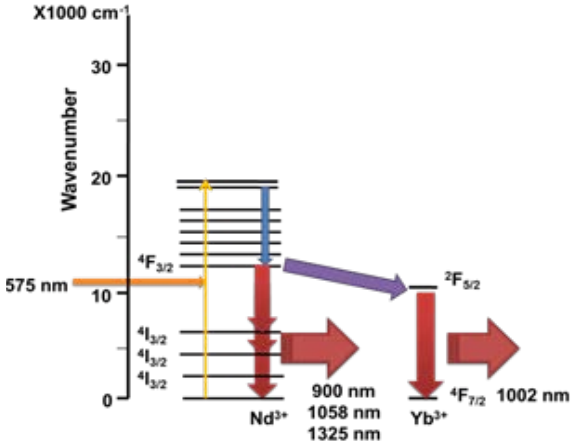

Fig. 5. Possible energy transfer mechanism of Nd^{3+} and Yb^{3+} codoped LaF_3 nanoparticles.

The energy level diagram is plotted for the Nd^{3+} and Yb^{3+} ions in **Fig. 5**. The Nd^{3+} ion is particularly rich in energy levels above 12000 cm^{-1} which are suitable for optical pumping. Fluorescence is frequently observed from the $^4F_{3/2}$ crystal levels of Nd^{3+}. The $^4F_{3/2}$ state is located only several hundred cm^{-1} above the $^2F_{5/2}$ state of Yb^{3+} so that energy could be transferred from Nd^{3+} to Yb^{+3} efficiently. This energy transfer was also observed in several other host lattices [**23, 30-35**].

Conclusion

OA-LaF_3 nanoparticles doped with Nd^{3+} and Yb^{3+} ions were synthesized. OA functionalization confirmed by FTIR & TGA studies. The OA-LaF_3: $Nd^{3+}Yb^{3+}$ nanoparticles ions were excited with 575 nm (at which Yb^{3+} cannot be excited) for understanding the energy transfer from Nd^{3+} to Yb^{3+}. The luminescence emission intensity from Nd^{3+} ions started to decrease as Yb^{3+} concentration increased. This could be attributed to the concentration quenching effect. The increase in the Yb^{3+} emission intensity was observed as Yb^{3+} dopant percentage increased up to 5%. Above 5% of Yb^{3+} co-doping with 10% Nd^{3+} both Nd^{3+} and Yb^{3+} luminescence observed to be decreasing which was attributed to the concentration quenching. LaF_3 singly doped with Yb^{3+} ions showed no excitation peaks between 400 nm to 800 nm for Yb^{3+} emission at 1002 nm. In the case of Yb^{3+} codoped with Nd^{3+} the excitation spectra for Yb^{3+} emission at 1002 nm, showed all the excitation peaks of Nd^{3+} ion in the visible region. This confirmed the sensitization of Yb^{3+} emission by Nd^{3+} ions.

Acknowledgements

The authors express thanks to SAIF-IIT-B for providing instrumental facilities for providing instrumental facilities (FTIR, TGA, HRTEM). Spectrofluorometer (FluoroLog-3, Horiba) was provided by DRDO.

Author's contributions

All authors are equally contributed. Authors have no competing financial interests.

References

1. Huang, X.; Han, S.; Huang, W.; Liu, X.; *Chem. Soc. Rev.*, **2013**, *42*, 173. **DOI:** 10.1039/C2CS35288E
2. Trupke, T.; Green, M.; Würfel, P.; *J. Appl. Phys.*, **2002**, *92*, 1668. **DOI:** 10.1063/1.1492021
3. Bünzli, J.-C. G.; Eliseeva, S. V.; *J. Rare Earths*, **2010**, *28*, 824. **DOI:** 10.1016/S1002-0721(09)60208-8
4. Bünzli, J.-C. G.; Piguet, C.; *Chem. Soc. Rev.*, **2005**, *34*, 1048. **DOI:** 10.1039/B406082M
5. Kumara P.; Gupta B. K.; *RSC Adv.*, **2015**, 5, 24729. **DOI:** 10.1039/C4RA15383A
6. Trupke, T.; Green, M.; Würfel, P.; *J. Appl. Phys*, **2002**, *92*, 4117. **DOI:** 10.1063/1.1492021
7. Yu D.;Rodríguez R.M.; Zhang Q.;Meijerink A.; Freddy T Rabouw; *Light Sci. Appl.*, **2015**, 4, e344 **DOI:** 10.1038/lsa.2015.117
8. Ru-Shi Liu (ED.); Phosphors, Up Conversion Nano Particles, Quantum Dots and Their Applications; Springer, 2016 **DOI:** 10.1007/978-3-662-52771-9
9. Taia Y.; Zhenga G.; Wanga H., Bai J.; *J. Solid State Chem.*, **2015**, 226, 250. **DOI:** 10.1016/j.jssc.2015.02.020
10. Zhang J.; Xia H.; Jiang Y.;Yang S.; Jiang H.;Zhang B.C.; *IEEE J. Quant. Electron.*, **2015**, 51,1. **DOI:** 10.1109/JQE.2015.2418756
11. Zhang, Q.; Yang, G.; Jiang, Z.; *Appl. Phys. Lett.*, **2007**, *91*, 1903. **DOI:** 10.1063/1.2757595
12. Huang, X.; Zhang, Q.; *J. Appl. Phys.*, **2009**, *105*, 53521. **DOI:** 10.1063/1.3088890
13. Meijer, J.-M.; Aarts, L.; van der Ende, B. M.; Vlugt, T. J.; Meijerink, A.; *Phys. Rev. B*, **2010**, *81*, 035107. **DOI:** 10.1103/PhysRevB.81.035107
14. Yu, D.; Ye, S.; Peng, M.; Zhang, Q.; Wondraczek, L.; *Appl. Phys. Lett.*, **2012**, *100*, 191911. **DOI:** 10.1063/1.4714505
15. Miritello, M.; Savio, R. L.; Cardile, P.; Priolo, F.; *Phys. Rev. B*, **2010**, *81*, 041411. **DOI:** 10.1103/PhysRevB.81.041411
16. Yu, D.; Huang, X.; Ye, S.; Peng, M.; Zhang, Q.; Wondraczek, L.; *Appl. Phys. Lett.*, **2011**, *99*, 161904. **DOI:** 10.1063/1.3652916
17. Batalioto, F.; de Sousa, D. F.; Bell, M. J. V.; Lebullenger, R.; Hernandes, A. C.; Nunes, L. A. O.; *J. Non-Cryst. Solids*, **2000**, *273*, 233. **DOI:** 10.1016/S0022-3093(00)00132-0
18. Lurin, C.; Parent C.; Le Flem G.; Hagenmuller P.; *J. Phys. Chem. Solids.*, **1985**, 46, 1083. **DOI:** 10.1016/0022-3697(85)90024-1
19. Parent C.; Lurin C.; Le Flem G.; Hagenmuller P.; *J Lumin.*, **1986**, 36, 49. **DOI:** 10.1016/0022-2313(86)90030-X
20. Ryba-Romanowski W.; Gołąb S.; Cichosz L.; Jeżowska-Trzebiatowska B.; *J. Non-Cryst. Solids.*, **1988**, 105, 295. **DOI:** 10.1016/0022-3093(88)90322-5
21. Batalioto F.; de Sousa DF.; Bell M. J. V.; Lebullenger R.; Hernandes A. C.; Nunes L. A. O.; *J. Non-Cryst. Solids.*, **2000**, 273, 233. **DOI:** 10.1016/S0022-3093(00)00132-0
22. De Sousa D, Batalioto F, Bell M, Oliveira S, Nunes L., *J. Appl. Phys.*, **2001**, 90, 3308. **DOI:** 10.1063/1.1397289
23. Rast H, Caspers H, Miller S. *J. Chem. Phys.*, **1967**, 47, 3874. **DOI:** 10.1063/1.1701548
24. Nampoothiri, P. K.; Gandhi, M. N.; Kulkarni, A., *J. Mater. Chem. C*, **2015**, *3*, 1817. **DOI:** 10.1039/C4TC02646B
25. Zhang, L.; He, R.; Gu, H.-C.; *Appl. Surf. Sci.*, **2006**, *253*, 2611. **DOI:** 10.1016/j.apsusc.2006.05.023
26. Wang, J.; Hu, J.; Tang, D.; Liu, X.; Zhen, Z.; *J. Mater. Chem.*, **2007**, 17, 1597. **DOI:** 10.1039/B617754A
27. Liu, G.; Conn, C. E.; Drummond, C. J.; *J. Phys. Chem. B*, **2009**, *113*, 15949. **DOI**: 10.1021/jp906344u
28. Deacon, G.; Huber, F.; Phillips, R.; *Inorg. Chim. Acta*, **1985**, *104*, 41. **DOI:** 10.1016/S0020-1693(00)83783-4
29. De Sousa, D.; Batalioto, F.; Bell, M.; Oliveira, S.; Nunes, L.; *J. Appl. Phys.*, **2001**, *90*, 3308. **DOI:** 10.1063/1.1397289
30. Jia, Z.; Arcangeli, A.; Tao, X.; Zhang, J.; Dong, C.; Jiang, M.; Bonelli, L.; Tonelli, M.; *J. Appl. Phys.*, **2009**, *105*, 083113. **DOI:** 10.1063/1.3115442
31. Liégard, F.; Doualan, J.; Moncorgé, R.; Bettinelli, M.; *Appl. Phys. B*, **2005**, *80*, 985. **DOI:** 10.1007/s00340-005-1829-y
32. Lurin, C.; Parent, C.; Le Flem, G.; Hagenmuller, P.; *J. Phys. Chem. Solids*, **1985**, *46*, 1083. **DOI:** 10.1016/0022-3697(85)90024-1
33. Miller, J.; Sharp, E.; *J. Appl. Phys.*, **1970**, *41*, 4718. **DOI:** 10.1063/1.1658520
34. Rast, H.; Caspers, H.; Miller, S.; *J. Chem. Phys.*, **1967**, *47*, 3874. **DOI:** 10.1063/1.1701548
35. Rivera-López, F.; Babu, P.; Basavapoornima, C.; Jayasankar, C.; Lavín, V.; *J. Appl. Phys.*, **2011**, *109*, 123514. **DOI:** 10.1063/1.3580475

